

On the evaluation of matrix elements in partially projected wave functions

Noboru Fukushima¹, Bernhard Edeger¹, V. N. Muthukumar², Claudius Gros¹

¹ Department of Physics, University of the Saarland, 66041 Saarbrücken, Germany and

² Department of Physics, City College at the City University of New York, New York, NY 10031

(Dated: October 8, 2018)

We generalize the Gutzwiller approximation scheme to the calculation of nontrivial matrix elements between the ground state and excited states. In our scheme, the normalization of the Gutzwiller wave function relative to a partially projected wave function with a single non projected site (the reservoir site) plays a key role. For the Gutzwiller projected Fermi sea, we evaluate the relative normalization both analytically and by variational Monte-Carlo (VMC). We also report VMC results for projected superconducting states that show novel oscillations in the hole density near the reservoir site.

I. INTRODUCTION

This paper concerns the calculation of matrix elements using projected wave functions of the form, $|\Psi\rangle = P|\Psi_0\rangle$. Here, $P = \prod_i (1 - n_{i\uparrow}n_{i\downarrow})$ is a projection operator which excludes double occupancies at sites i , and $|\Psi_0\rangle$, a trial wave function. Projected wave functions of this form were originally proposed by Gutzwiller to study electronic systems with repulsive on-site interactions¹. The choice of $|\Psi_0\rangle$ depends on the problem under consideration. For instance, a projected Fermi liquid state,

$$P|\Psi_{\text{FS}}\rangle = P \prod_{k < k_F} c_{k\uparrow}^\dagger c_{k\downarrow}^\dagger |0\rangle, \quad (1)$$

was used successfully in the description of liquid ^3He as an almost localized Fermi liquid^{2,3}. Soon after the discovery of high temperature superconductivity in the cuprates, projected BCS wave functions were proposed as possible ground states of the so-called $t - J$ model^{4,5}. Early results from variational Monte Carlo (VMC) studies as well as a renormalized mean field theory based on Gutzwiller approximation showed that a projected d -wave BCS state,

$$P_N P |\Psi_{\text{BCS}}\rangle = P_N P \prod_k \left(u_k + v_k c_{k\uparrow}^\dagger c_{-k\downarrow}^\dagger \right) |0\rangle, \quad (2)$$

reproduces many features seen in the phase diagram of the high temperature superconductors^{6,7,8}. The projection operator P_N which fixes the particle number N in (2), is useful when considering the phase diagram near half filling⁶. Without P_N in (2), one would need to consider the effects of particle number fluctuations, which become singular near half-filling^{9,10}.

Detailed VMC studies have been carried out recently using projected d -wave BCS states as variational wave functions for the two dimensional Hubbard model¹¹, after a suitable canonical transformation³. Similar wave functions have been proposed in the literature for cobaltate superconductors as well as organic superconductors^{12,13}. To make analytical progress however, it is desirable to extend Gutzwiller's scheme and construct normalized single particle excitations and calculate matrix elements. In this paper, we take the first step in this direction. We

construct normalized excitations of the Gutzwiller projected Fermi sea and consider the evaluation of matrix elements.

In his original paper, Gutzwiller proposed that in calculating expectation values of operators with projected wave functions, the effects of projection on the state $|\Psi_0\rangle$ could be approximated by a classical statistical weight factor, which multiplies the quantum result¹⁴. Thus, for example,

$$\frac{\langle \Psi | \hat{O} | \Psi \rangle}{\langle \Psi | \Psi \rangle} \approx g \frac{\langle \Psi_0 | \hat{O} | \Psi_0 \rangle}{\langle \Psi_0 | \Psi_0 \rangle}, \quad (3)$$

where \hat{O} is any operator, and g , a statistical weight factor. The basic idea is that the projection operator P reduces the number of allowed states in the Hilbert space, and invoking a simple approximation, such a reduction can be taken into account through combinatorial factors. For example, expectation values of the the kinetic energy operator $c_i^\dagger c_j + c_j^\dagger c_i$ and the superexchange interaction between sites i and j , $\vec{S}_i \cdot \vec{S}_j$ in the projected subspace of states are renormalized by the Gutzwiller factors,

$$g_t = \frac{1 - n}{1 - n/2}, \quad g_s = \frac{1}{(1 - n/2)^2}, \quad (4)$$

where n is the density of electrons. In deriving these renormalization factors, one considers the number of states that contribute to $\langle \Psi | \hat{O} | \Psi \rangle$ and to $\langle \Psi_0 | \hat{O} | \Psi_0 \rangle$ respectively. The ratio of these two contributions is identified as the renormalization factor.

It is clear that this approach can be generalized to evaluate matrix elements of an operator \hat{O} between different projected states. However, as we will see in this paper, many of the matrix elements that are of interest are reduced to the calculation of matrix elements between partially projected wave functions of the form

$$|\Psi'_l\rangle = P'_l |\Psi_0\rangle, \quad P'_l = \prod_{i \neq l} (1 - n_{i\uparrow}n_{i\downarrow}). \quad (5)$$

The wave function $|\Psi'_l\rangle$ describes a state where double occupancies are projected out on all sites except the site l , which we call the reservoir site. The reason for the appearance of reservoir sites is not far to seek. Consider, for

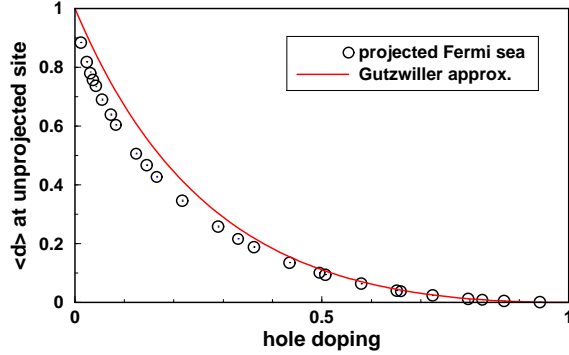


FIG. 1: Double occupancy of the reservoir site, $\langle n_\uparrow n_\downarrow \rangle_{\Psi'_l} = 1 - X$, as a function of doping, for the partially projected Fermi sea. See (6) and (1). Note the good agreement between the Gutzwiller result (solid line), Eqs. (10,15) and the VMC results for the projected Fermi sea (open circles). Statistical errors and finite-size corrections are estimated to be smaller than the symbols.

example, the operator $P_{l\uparrow}$. Clearly, it can be rewritten as $c_{l\uparrow}P'_l$. Since calculation of matrix elements involving excited states involve the commutation of projection operators with creation/destruction operators, partially projected states arise inevitably within the Gutzwiller scheme.

In this paper, we present a method to calculate matrix elements between a partially projected Fermi sea, *i.e.*, a projected Fermi sea with a reservoir site at l , as in (5). We will show that this problem has to be solved if we were to construct normalized particle/hole excitations of the (fully) projected Fermi sea. The same problem arises when calculating matrix elements for particle/hole tunneling into the projected Fermi sea. We develop an analytical approximation to solve this problem, and use it to calculate various matrix elements. We use VMC to test the validity of the approximation and find that our analytical results for the partially projected Fermi sea are in good agreement with the results from VMC.

The outline of the paper is as follows. In Sec. II, we present results for the occupancy of the reservoir site. We use these results in Sec. III, where we show how normalized single particle excitations can be constructed from the projected Fermi sea. In Sec. IV we calculate the matrix elements for particle/hole tunneling into the projected Fermi sea. VMC results for density oscillations in the vicinity of the reservoir site for both projected Fermi sea and BCS states are presented in Sec. V. The final section contains a summary and discussion of results.

II. OCCUPANCY OF THE RESERVOIR SITE

Consider a partially projected wave function,

$$|\Psi'_l\rangle = P'_l|\Psi_0\rangle, \quad P'_l = \prod_{i \neq l} (1 - n_{i\uparrow}n_{i\downarrow}). \quad (6)$$

Double occupancy is projected out on all sites except the site l , called the reservoir site. Unless specified otherwise, we take $|\Psi_0\rangle$ to mean the Fermi sea. For the calculation of single particle excitations and matrix elements, we need expectation values such as

$$\frac{\langle \Psi'_l | \hat{O} | \Psi'_l \rangle}{\langle \Psi'_l | \Psi'_l \rangle} = g' \frac{\langle \Psi_0 | \hat{O} | \Psi_0 \rangle}{\langle \Psi_0 | \Psi_0 \rangle}, \quad (7)$$

that generalize the Gutzwiller renormalization scheme (3) to partially projected wave functions.

A. Gutzwiller approximation

In order to evaluate the generalized renormalization parameters g' in (7), we obviously need the normalization $\langle \Psi'_l | \Psi'_l \rangle$. We define

$$X = \frac{\langle \Psi_0 | PP | \Psi_0 \rangle}{\langle \Psi_0 | P'_l P'_l | \Psi_0 \rangle} = \frac{\langle \Psi | \Psi \rangle}{\langle \Psi'_l | \Psi'_l \rangle}, \quad (8)$$

the norm of the fully projected state relative to the state with one reservoir site. Invoking the Gutzwiller approximation, we estimate this ratio by considering the relative sizes of the Hilbert spaces,

$$X \sim \frac{\frac{L!}{N_\uparrow! N_\downarrow! N_h!}}{\frac{L!}{N_\uparrow! N_\downarrow! N_h!} + \frac{(L-1)!}{(N_\uparrow-1)!(N_\downarrow-1)!(N_h+1)!}}, \quad (9)$$

where $L = N_\uparrow + N_\downarrow + N_h$, is the number of lattice sites, N_\uparrow , N_\downarrow and N_h , the number of up spins, down spins and empty sites respectively. The first term in the denominator of (9) represents the number of states with the reservoir site being empty or singly occupied; the second term represents the state with the reservoir site being doubly occupied.

Eq. (9) can be simplified in the thermodynamic limit. We get,

$$X = \frac{1 - n}{(1 - n_\uparrow)(1 - n_\downarrow)}, \quad (10)$$

where the particle densities, $n_\sigma = N_\sigma/L$ ($\sigma = \uparrow, \downarrow$) and $n = n_\uparrow + n_\downarrow$. The above argument can be extended to the case of two unprojected sites in an otherwise projected Fermi sea. We then get,

$$\frac{\langle \Psi_0 | PP | \Psi_0 \rangle}{\langle \Psi_0 | P'_{lm} P'_{lm} | \Psi_0 \rangle} = X^2, \quad (11)$$

where, $P_{lm} = \prod_{i \neq l, m} (1 - n_{i\uparrow}n_{i\downarrow})$. We note for later use that

$$\frac{1 - X}{X} = \frac{n_\uparrow n_\downarrow}{(1 - n)}. \quad (12)$$

B. Exact relations

Assuming translation invariance, it is possible to derive the following exact expressions

$$\langle (1 - n_{l\uparrow})(1 - n_{l\downarrow}) \rangle_{\Psi'_l} = X(1 - n) \quad (13)$$

$$\langle n_{l\sigma}(1 - n_{l-\sigma}) \rangle_{\Psi'_l} = Xn_\sigma \quad (14)$$

$$\langle d \rangle_{\Psi'_l} \equiv \langle n_{l\uparrow}n_{l\downarrow} \rangle_{\Psi'_l} = 1 - X \quad (15)$$

for the occupancy of the reservoir site, where

$$\langle \dots \rangle_{\Psi'_l} \equiv \langle \Psi'_l | \dots | \Psi'_l \rangle / \langle \Psi'_l | \Psi'_l \rangle .$$

The proof is straightforward. Consider for instance, the probability (13) of finding the reservoir site empty. Since,

$$\begin{aligned} \langle \Psi_0 | P(1 - n_l)P | \Psi_0 \rangle \\ = \langle \Psi_0 | P'_l(1 - n_{l\uparrow})(1 - n_{l\downarrow})P'_l | \Psi_0 \rangle \end{aligned} \quad (16)$$

we have,

$$\begin{aligned} \langle (1 - n_{l\uparrow})(1 - n_{l\downarrow}) \rangle_{\Psi'_l} \\ = \frac{\langle \Psi | (1 - n_l) | \Psi \rangle}{\langle \Psi | \Psi \rangle} \frac{\langle \Psi | \Psi \rangle}{\langle \Psi'_l | \Psi'_l \rangle} = (1 - n)X . \end{aligned}$$

Eqs. (14) and (15) can be proved analogously.

C. VMC results for projected Fermi sea and BCS states

In Fig. 1, we compare (10) with VMC results for $\langle d \rangle_{\Psi'_l} = 1 - X$. We find that the results from the generalized Gutzwiller approximation are in excellent qualitative agreement with the VMC results for a partially projected Fermi sea. We also used VMC to obtain the same quantity using projected *s/d*-wave BCS states as variational states in the simulation. The results for $\langle d \rangle_{\Psi'_l}$ in BCS states are shown in Fig. 2. In contrast to the projected Fermi sea, a clear deviation from the Gutzwiller approximation is seen. This underscores the importance of pairing correlations in the unprojected wave function that are not completely taken into account by the Gutzwiller approximation scheme. These differences between Fermi sea and BCS states are discussed in more detail in Sect. V, where we consider density oscillations in the vicinity of the reservoir site.

In the following we discuss some details of the VMC calculations with one unprojected (reservoir) site l . As mentioned earlier, single occupancy is enforced (by projection) on all other sites. Simulations are performed on a finite square lattice spanned by two vectors (L_x, L_y) and $(-L_y, L_x)$ with periodic boundary conditions¹⁶. The number of sites, $L = L_x^2 + L_y^2$. The numbers of up- and down-electrons are chosen to be equal, $N_\uparrow = N_\downarrow$. The simulation for the local quantity $\langle d \rangle_{\Psi'_l} = \langle n_{l\uparrow}n_{l\downarrow} \rangle_{\Psi'_l}$ has a larger statistical error than results for macroscopic quantities in uniform systems because the summation over site

indices yields effectively L times more statistics for the latter. In order to overcome this problem, we update the reservoir site more often than the projected sites. Accordingly, the transition probability needs an extra weighting factor to keep the local balance. With this procedure, we can improve the statistical accuracy by about one order of magnitude. In addition, we carry out measurements after every update. Usually, in VMC simulations, measurement are performed every $O(L)$ updates to obtain independent samples since similar states return similar sampled data. However, in the case of $n_{l\uparrow}n_{l\downarrow}$, a measurement returns only 0 or 1; *viz.*, the sampled data can be different even when the states are similar. Given this, the measurement after every update seems more reasonable as it reduces statistical errors. Furthermore, we have restricted updates to the transfer of a single electron to an unoccupied site, and excluded updates *via* the exchange of two electrons. The calculation of the transition probabilities for the former update consumes time of $O(N_\sigma)$ whereas the time taken for the latter update is $O(N_\sigma^2)$. As the system size increases, this restriction achieves efficiency. We have collected statistics from up to 60 independent runs over two days, and the total number of updates amounts to $10^8 \sim 10^9$.

For superconducting states, one can perform the VMC simulation either with fixed particle number $P_N P | \Psi_{\text{BCS}} \rangle$, or with a fixed phase $P | \Psi_{\text{BCS}} \rangle$ ^{10,16}. For the latter choice, particle number fluctuation hinders the variational wave function from reaching half filling unless the chemical potential μ goes to infinity. On the other hand, the wave function can be optimized by varying the gap Δ_k even at half filling, if we choose to fix the particle number. It is important to note that simulations with fixed particle number are done not with the most probable N of $P | \Psi_{\text{BCS}} \rangle$, but that of $| \Psi_{\text{BCS}} \rangle$. This is because P decreases the average particle number¹⁰. Despite these differences, both choices of wave functions yield quantitatively similar results¹⁰. Throughout this paper we choose to fix the particle number while working with projected BCS states.

Let us define $a_k \equiv v_k/u_k$. For the *d*-wave BCS state, $a_{k=0} = 0$ in the thermodynamic limit. However, if one chooses $a_{k=0} = 0$ in the finite system, the $k = 0$ state is unoccupied, although it is the lowest energy state. One can also choose a large value for $a_{k=0}$. Usually, the difference between these choices is $O(1/N)$. We expect an N electron system with $a_{k=0} = 0$ to be similar to an $N + 2$ electron system with large $a_{k=0}$, because the two electrons that are no longer in the $k = 0$ state can occupy other available states. However, this argument fails at half filling for projected states, because there are no available states left for the two extra electrons. So it should not be surprising that X depends strongly on these choices close to half filling; the $a_{k=0} = 0$ definition gives larger X than the other does as shown in Fig. 3. At the other fillings, our results show only $O(1/N)$ of difference between these choices. Except for Fig. 3, where we show both cases, all other results in this paper are ob-

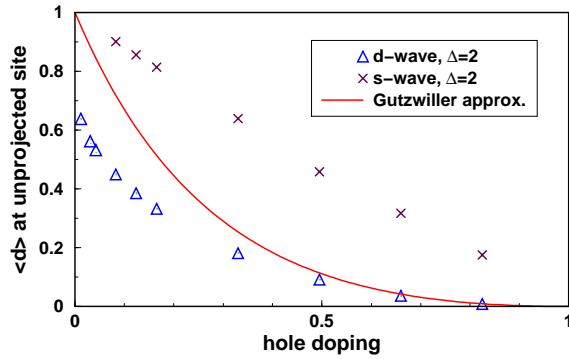


FIG. 2: Double occupancy at the reservoir site $\langle n_\uparrow n_\downarrow \rangle_{\Psi_i} = 1 - X$, as a function of doping, for the partially projected BCS wave function, see (6) and (2). The parameterization follows Ref. 16. Statistical errors and finite-size corrections are estimated to be smaller than the symbols.

tained for a choice of large $a_{k=0}$; *i.e.*, we take $a_{k=0}$ larger than any other a_k .

The system size dependence is quite small except in the vicinity of half filling. In fact, it is qualitatively consistent with the Gutzwiller approximation; size dependence enters only as $(N_h + 1)/L$ in Eq. (9) and is negligible for large N_h . In Fig. 3, we show the dependence of $\langle d \rangle$ on the system size. As shown in Fig. 3, $\langle d \rangle$ approaches unity for the projected Fermi sea. For the projected *d*-wave BCS state, we speculate that the value of $\langle d \rangle$ goes to unity too, because it does not saturate, but increases more rapidly as $1/L$ decreases.

III. SINGLE PARTICLE EXCITATIONS OF THE PROJECTED FERMI SEA

We consider the particle excitation

$$|\Psi_{k\sigma}^+\rangle = P c_{k\sigma}^\dagger |\Psi_0\rangle, \quad (17)$$

and the hole excitation

$$|\Psi_{k\sigma}^-\rangle = P c_{k\sigma} |\Psi_0\rangle. \quad (18)$$

Any calculation involving $|\Psi_{k\sigma}^\pm\rangle$ needs the respective norms, $N_{k\sigma}^\pm = \langle \Psi_{k\sigma}^\pm | \Psi_{k\sigma}^\pm \rangle$. We now calculate these norms within the generalized Gutzwiller approximation.

A. Particle excitation

For the particle excitation, we get,

$$\frac{N_{k\sigma}^+}{N_G} = 1 - n + g_t (n_\sigma - n_{k\sigma}^0) = g_t (1 - n_{k\sigma}^0), \quad (19)$$

where $g_t = (1 - n)/(1 - n_\sigma)$, $N_G = \langle \Psi | \Psi \rangle$, and $n_{k\sigma}^0 = \langle c_{k\sigma}^\dagger c_{k\sigma} \rangle_{\Psi_0}$ is the momentum distribution function in the unprojected site.

Equation (19) has appeared frequently in the literature. here, we repeat its derivation to facilitate a comparison with the analogous problem for hole excitations. The norm $\langle \Psi_{k\sigma}^+ | \Psi_{k\sigma}^+ \rangle$ is given by

$$\begin{aligned} N_{k\sigma}^+ &= \langle \Psi_0 | c_{k\sigma} P P c_{k\sigma}^\dagger | \Psi_0 \rangle = \frac{1}{L} \sum_{l,m} e^{ik(l-m)} \langle \Psi_0 | P'_l (1 - n_{l-\sigma}) c_{l\sigma} c_{m\sigma}^\dagger (1 - n_{m-\sigma}) P'_m | \Psi_0 \rangle \\ &= \frac{1}{L} \sum_l \langle \Psi_0 | P'_l (1 - n_{l\sigma}) (1 - n_{l-\sigma}) P'_l | \Psi_0 \rangle + \frac{1}{L} \sum_{l \neq m} e^{ik(l-m)} \langle \Psi_0 | P c_{l\sigma} c_{m\sigma}^\dagger P | \Psi_0 \rangle \\ &= N_G \frac{\langle \Psi | (1 - n) | \Psi \rangle}{\langle \Psi | \Psi \rangle} - \frac{N_G}{L} \sum_{l \neq m} e^{ik(l-m)} \frac{\langle \Psi | c_{m\sigma}^\dagger c_{l\sigma} | \Psi \rangle}{\langle \Psi | \Psi \rangle}, \end{aligned} \quad (20)$$

where we have used (16) for the diagonal contribution in the last step. Invoking the Gutzwiller approximation for the off-diagonal term, Eq. (19) follows directly from (20).

B. Hole excitation

The normalization of the hole excitation can be done analogously. We get,

$$\frac{N_{k\sigma}^-}{N_G} = \frac{1}{N_G L} \sum_{l,m} e^{ik(l-m)} \langle \Psi_0 | P'_l c_{l\sigma}^\dagger c_{m\sigma} P'_m | \Psi_0 \rangle = \frac{1}{X} [X n_\sigma + (1 - X)] + \frac{1}{N_G L} \sum_{l \neq m} e^{ik(l-m)} \langle \Psi_0 | P'_{lm} c_{l\sigma}^\dagger c_{m\sigma} P'_{lm} | \Psi_0 \rangle,$$

where, $P_{lm} = \prod_{i \neq l,m} (1 - n_{i,\uparrow} n_{i,\downarrow})$. The last term in the above equation corresponds to a hopping process between two reservoir sites. The generalized Gutzwiller approximation assumes that the matrix elements are proportional to the square roots of the corresponding densities (13,14,15).

Invoking the Gutzwiller approximation and using (11), we get,

$$\frac{N_{k\sigma}^-}{N_G} = \frac{\langle \Psi_{k\sigma}^- | \Psi_{k\sigma}^- \rangle}{\langle \Psi | \Psi \rangle} = n_\sigma + \frac{1-X}{X} + \frac{n_{k\sigma}^0 - n_\sigma}{X^2 n_\sigma (1-n_\sigma)} \left[\sqrt{X(1-n)} \sqrt{X n_\sigma} + \sqrt{X n_{-\sigma}} \sqrt{1-X} \right]^2, \quad (21)$$

for the normalization of the hole excitation relative to the norm of the Gutzwiller wave function.

The general expression (21) for the hole normalization, can be simplified upon using the Gutzwiller result (12) for the relative norm X . We then get,

$$\frac{n_{k\sigma}^0 - n_\sigma}{n_\sigma (1-n_\sigma)} \left[\sqrt{1-n} \sqrt{n_\sigma} + \sqrt{n_{-\sigma}} \sqrt{(1-X)/X} \right]^2 = (n_{k\sigma}^0 - n_\sigma) \frac{[(1-n) + n_{-\sigma}]^2}{(1-n_\sigma)(1-n)} = (n_{k\sigma}^0 - n_\sigma) \frac{1-n_{-\sigma}}{(1-n)},$$

for the last term in (21). Finally, we get the simple result,

IV. TUNNELING MATRIX ELEMENTS

$$\frac{N_{k\sigma}^-}{N_G} = n_{k\sigma} \frac{1-n_{-\sigma}}{(1-n)} = \frac{n_{k\sigma}}{g_t} \quad (22)$$

It is interesting to compare this result for the normalization of the hole excitation with the corresponding expression (19) for the particle excitation. The vanishing of the latter at half filling could have been expected. But the divergence of $N_{k\sigma}^-$ as $n \rightarrow 1$ is surprising. We will return to this point in the next section.

C. Consistency check

The norm $N_{k\sigma}^+$ has to vanish whenever $|\Psi_{k\sigma}^+\rangle = P c_{k\sigma}^\dagger |\Psi_0\rangle$ vanishes. For the Fermi sea this is the case when $k < k_F$, i.e. when $n_{k\sigma}^0 = 1$. This physical condition is obviously fulfilled by (19). Similarly, we expect $N_{k\sigma}^-$ to vanish for $n_{k\sigma}^0 = 0$, which is satisfied by (22). Thus, the Gutzwiller result (10) obeys the normalization condition for the hole excitation and the theory is consistent.

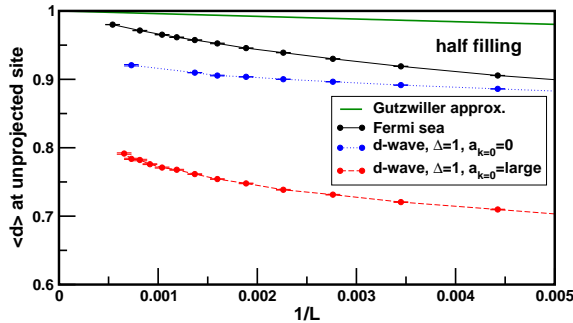


FIG. 3: The size dependence of the double occupancy at the reservoir site, (15), at half filling. The VMC result for the Gutzwiller state (upper curve) seems to converge nicely to unity in the thermodynamic limit, in agreement with Eqs. (10) and (12). The results for the projected d -wave show a pronounced dependence on the occupancy of the $k = 0$ state. See text for details.

We now consider the tunneling of electrons and holes into a projected wave function. Single particle tunneling into a projected superconducting state has been considered recently by Anderson and Ong⁹, and Randeria *et al.*¹⁵. Here, we restrict ourselves to the projected Fermi liquid state and evaluate the tunneling matrix elements by retaining systematically, all terms arising from the commutation of the electron creation and destruction operators with the projection operator P , as outlined in Sec. III.

A. Particle tunneling

Consider first, the matrix element

$$M_{k\sigma}^+ = \frac{\left| \langle \Psi_{k\sigma}^+ | c_{k\sigma}^\dagger | \Psi \rangle \right|^2}{N_{k\sigma}^+ N_G}. \quad (23)$$

The numerator may be calculated easily by using the result of (19):

$$\begin{aligned} \langle \Psi_0 | c_{k\sigma} P c_{k\sigma}^\dagger P | \Psi_0 \rangle &= \frac{\langle \Psi_0 | c_{k\sigma} P P c_{k\sigma}^\dagger | \Psi_0 \rangle}{N_G} \\ &= g_t (1 - n_{k\sigma}^0). \end{aligned}$$

From the above expression we find that the particle tunneling matrix element takes the form,

$$M_{k\sigma}^+ = \frac{g_t^2 (1 - n_{k\sigma}^0)^2}{g_t (1 - n_{k\sigma}^0)} = g_t (1 - n_{k\sigma}^0). \quad (24)$$

It vanishes at half filling $n \rightarrow 1$, implying that the *addition* of electrons is not possible exactly at half filling because of the restriction in the Hilbert space.

B. Hole tunneling

Next we evaluate the matrix element

$$M_{k\sigma}^- = \frac{\left| \langle \Psi_{k\sigma}^- | c_{k\sigma} | \Psi \rangle \right|^2}{N_{k\sigma}^- N_G}, \quad (25)$$

corresponding to the tunneling of holes into the projected state. Naively, we might expect this process to be allowed at half filling, since the *removal* of electrons is not forbidden by the projection operator. Consider now, the

matrix element in the numerator of (25). We follow the same procedure used to evaluate the norm of the hole wave function in Sec. III B and use (12) and (14) and find,

$$\begin{aligned}
\frac{\langle \Psi_0 | c_{k\sigma}^\dagger P c_{k\sigma} P | \Psi_0 \rangle}{N_G} &= \frac{1}{N_G L} \sum_{l,m} e^{ik(l-m)} \langle \Psi_0 | P'_l c_{l\sigma}^\dagger c_{m\sigma} P | \Psi_0 \rangle = \frac{X n_\sigma}{X} + \frac{1}{N_G L} \sum_{l \neq m} e^{ik(l-m)} \langle \Psi_0 | P'_l c_{l\sigma}^\dagger c_{m\sigma} P'_l | \Psi_0 \rangle \\
&= \frac{X n_\sigma}{X} + (n_{k\sigma}^0 - n_\sigma) \frac{\left[\sqrt{X n_{-\sigma}} \sqrt{1-X} + \sqrt{X(1-n)} \sqrt{X n_\sigma} \right] \sqrt{1-n} \sqrt{n_\sigma}}{X(1-n_\sigma) n_\sigma} \\
&= n_\sigma + (n_{k\sigma}^0 - n_\sigma) \frac{n_{-\sigma} n_\sigma + (1-n) n_\sigma}{(1-n_\sigma) n_\sigma} = n_{k\sigma}^0.
\end{aligned} \tag{26}$$

Using this expression together with the norm (21) of the hole excitation, we obtain the hole tunneling matrix element (25),

$$M_{k\sigma}^- = \frac{n_{k\sigma}^0 n_{k\sigma}^0}{n_{k\sigma}^0 / g_t} = g_t n_{k\sigma}^0, \tag{27}$$

a surprising result, in that it vanishes at half filling ($n_\uparrow = n_\downarrow = 0.5$) too.

The vanishing of the hole tunneling matrix element at half filling is clearly related to the divergence of the norm of the hole excitation. This, in turn, is related to the fact that $X \rightarrow 0$, as $n \rightarrow 1$ (cf. Eq(10)). The vanishing hole tunneling matrix element can then be understood as follows. When the reservoir site is doubly occupied, a single hole in the otherwise projected Fermi sea can be found in any of the lattice sites. Consequently, when double occupancy of the reservoir site occurs with probability 1, as it does at half filling, an “orthogonality catastrophe” occurs leading to zero overlap for the tunneling matrix element. Note that the result (27) hinges on the exact functional dependence (12) of $(1-X)/X$ on the particle densities n_σ . On the other hand, the particle tunneling matrix element $M_{k\sigma}^+$ is not affected by the functional form of the relative normalization factor X . If X were to vanish more slowly than $(1-n)$ at half filling, then from (21) and (26), one could conclude that the hole tunneling matrix element $M_{k\sigma}^-$ does not vanish as $n \rightarrow 1$, possibly leading to an asymmetry between particle and hole tunneling. Our analytical results preclude this possibility for the projected Fermi sea. But we are unable to provide a definite answer for the projected superconducting states, in view of the discrepancy between the Gutzwiller approximation and the VMC results (Fig. 2). To understand this discrepancy, we study density oscillations in the vicinity of the reservoir site using VMC.

V. DENSITY OSCILLATIONS NEAR THE RESERVOIR SITE

To clarify the limitations of the Gutzwiller approximation for projected superconducting states, we use VMC to calculate the hole density in the vicinity of the reservoir site. We find that the density oscillations seen are very different for the projected Fermi sea and the BCS states.

Fig. 4 shows VMC results for the hole density

$$n_h(m) = \langle 1 - n_m \rangle_{\Psi'_l},$$

in the partially projected state $|\Psi'_l\rangle$ are presented in the first row of. The sites m are distinct from the reservoir site l (marked by a cross in the figure). All results shown correspond to half filling; *viz.*, $n_\uparrow = n_\downarrow = 0.5$. We choose $\Delta = 1$ for the BCS states. The vectors of periodic boundary conditions are $\vec{L}_1 = (L_x, L_y)$ and $\vec{L}_2 = (-L_y, L_x)$ respectively, with $L_x = 37, L_y = 1$; Including the reservoir site, $L = L_x^2 + L_y^2 = 1370$ sites. In the figure, white/black correspond to high/low values of $n_h(m)$, which is scaled by a logarithmic gray scale varying in the range $-8.5 < \log n_h(m) < -6$. Thus, the same gray represents the same value in all the three cases shown.

For the Fermi sea, we see that the hole is distributed more uniformly than the other cases even though the diagonal direction has a larger probability of being occupied by a hole. The s -wave shows a checker-board pattern. The d -wave has a quasi checker-board pattern where only one of four sites is black, and the hole tends to be near the reservoir site. The VMC results for the projected BCS wave functions are strikingly different in that the hole density is *not* uniform. On the other hand, the Gutzwiller approximation would be exact, if all states in the Hilbert space contribute equally to the wave function. That would correspond to a uniform density of holes. Clearly, the Gutzwiller approximation has to be

extended to treat projected superconducting wave functions. This is in agreement with our previous considerations, where we found that the functional form of X (Eq. 10, derived using Gutzwiller approximation) agrees with the VMC calculations only for the projected Fermi sea, but not for BCS states (see Fig. 1 and Fig. 2).

To further investigate the effects of Gutzwiller projection, we also plot (second row of Fig. 4) the correlation function

$$d_h^{(0)}(m) = \langle n_{l\uparrow} n_{l\downarrow} (1 - n_{m\uparrow}) (1 - n_{m\downarrow}) \rangle \quad (28)$$

$$- \langle n_{l\uparrow} n_{l\downarrow} \rangle \langle (1 - n_{m\uparrow}) (1 - n_{m\downarrow}) \rangle$$

in systems *without* the Gutzwiller projection. This correlations function between a hole at site m and a doubly occupied site at l corresponds to the quantity $n_h(m)$ for the partially projected wave function close to half filling. This is because, in the latter case, the unprojected site is doubly occupied. Note that translation invariance implies that the second term in (28) does not depend on the site indices l and m , and is a constant factor. Then, using Wick's theorem, the correlation function $d_h^{(0)}(m)$ is reduced to a function of $\langle c_{i,\uparrow}^\dagger c_{j,\uparrow} \rangle$ and $\langle c_{i,\uparrow} c_{j,\downarrow} \rangle$. The quantity $d_h^{(0)}(m)$ can be evaluated exactly, performing a Fourier transform (we use the same system size and boundary conditions). The logarithm of the correlation function is scaled in the second row of Fig. 4 by the gray scale varying in the range $(-22, -4)$. Both $\langle c_{i,\uparrow}^\dagger c_{j,\uparrow} \rangle$ and $\langle c_{i,\uparrow} c_{j,\downarrow} \rangle$ show Friedel oscillations.

For the Fermi sea, only $\langle c_{i,\uparrow}^\dagger c_{j,\uparrow} \rangle$ is finite. The nesting of the Fermi surface by $Q = (\pi, \pi)$ then leads to the checker-board pattern for the hole density observed in Fig. 4 (second row).

For the s -wave, the Friedel oscillations of $\langle c_{i,\uparrow}^\dagger c_{j,\uparrow} \rangle$ are similar to that of the Fermi sea while the oscillation of $\langle c_{i,\uparrow} c_{j,\downarrow} \rangle$ is phase shifted by $\pi/2$. Summing both contributions to $d_h^{(0)}(m)$ the oscillations are smeared out. In contrast, for the d -wave both $\langle c_{i,\uparrow}^\dagger c_{j,\uparrow} \rangle$ and $\langle c_{i,\uparrow} c_{j,\downarrow} \rangle$ oscillate in phase, leading to the oscillation observed.

Let us compare these results with those obtained after projection. For the Fermi sea, we see clearly that the density oscillations are suppressed by projection. This is likely because projection reduces the discontinuity at the Fermi level, thereby suppressing the nesting by Q and the corresponding Friedel oscillations.

The emergence of the checker-board pattern in the projected s -wave suggests that Gutzwiller projection affects $\langle c_{i,\uparrow} c_{j,\downarrow} \rangle$ stronger than $\langle c_{i,\uparrow}^\dagger c_{j,\uparrow} \rangle$. With only one contribution, the Friedel oscillations are no longer smeared out and are observed.

Projection changes the pattern qualitatively for the d -wave too. The observed pattern resembles approximately the function, $\sim \sin^2(x\pi/2) \sin^2(y\pi/2)$ (see Fig. 4, top row), with $m = (x, y)$. This indicates that the nodal points at $(\pm\frac{\pi}{2}, \pm\frac{\pi}{2})$ contribute dominantly after projection. Furthermore, in this case, the hole tends to stay near the reservoir site. It means that only a part of the

Hilbert space has a large weight, leading to a deviation from the Gutzwiller approximation. We believe this effect cannot be captured within the Gutzwiller approximation without invoking off-site correlations¹⁷.

VI. DISCUSSION

In this paper, we extended the Gutzwiller approximation scheme to construct normalized excitations and matrix elements for the projected Fermi sea. In typical calculations, one needs to determine matrix elements between partially projected Gutzwiller projected states, where double occupancies are projected out at all but one site l (called the “reservoir” site). The occupancy of the reservoir site, n_l turns out to be an important quantity in the calculation of matrix elements. Since the wave function projects out double occupancies on all sites $m \neq l$, it follows that the occupancy $n_m \leq 1$. But, $n_l = \{0, 1, 2\}$. Therefore, our results for n_l are nontrivial in that the Gutzwiller approximation is extended to calculate the occupancy at an *unprojected* site. We presented an analytical method to calculate such matrix elements and showed that the approximations are in good agreement with results from variational Monte Carlo (VMC) for the Fermi sea. These results were used to construct normalized single particle excitations of the fully projected Fermi sea, and to calculate matrix elements for tunneling into the projected Fermi sea.

Single particle tunneling in projected BCS wave functions has been discussed recently, by Anderson and Ong⁹, and Randeria *et al.*¹⁵. In our calculations for tunneling into the projected Fermi sea, we find the surprising result that the matrix elements for both particle and hole tunneling vanish as $n \rightarrow 1$ (half filling). Within our scheme, the result follows from the behavior of the charge density in the vicinity of the reservoir site. In particular, for the projected Fermi sea the analytical result hinges on the expression for single occupancy of the reservoir site, Eq. (10). As can be seen in Fig. 2, the analytical result does not agree with numerical calculations done for projected BCS wave functions. This discrepancy underscores the importance of pairing correlations in the unprojected wave functions, which are not taken into account within the Gutzwiller approximation scheme.

There are two ways by which electron correlations arise in the Gutzwiller scheme: one is through the mean field or trial wave function $|\Psi_0\rangle$, and the other *via* the projection on the subspace of no double occupancy, $|\Psi\rangle = P|\Psi_0\rangle$. The latter effect, which results in the reduction in the size of the Hilbert space can be described by combinatorial arguments, leading to (10). As seen in Fig. 1, the analytical and VMC results are in good agreement for the case of the projected Fermi sea. We can trace this agreement back to the fact that the Fermi sea does not contain any additional explicit correlations.

Consider instead $|\Psi_{\text{BCS}}\rangle$, which contains additional, molecular field correlations in the unprojected wave func-

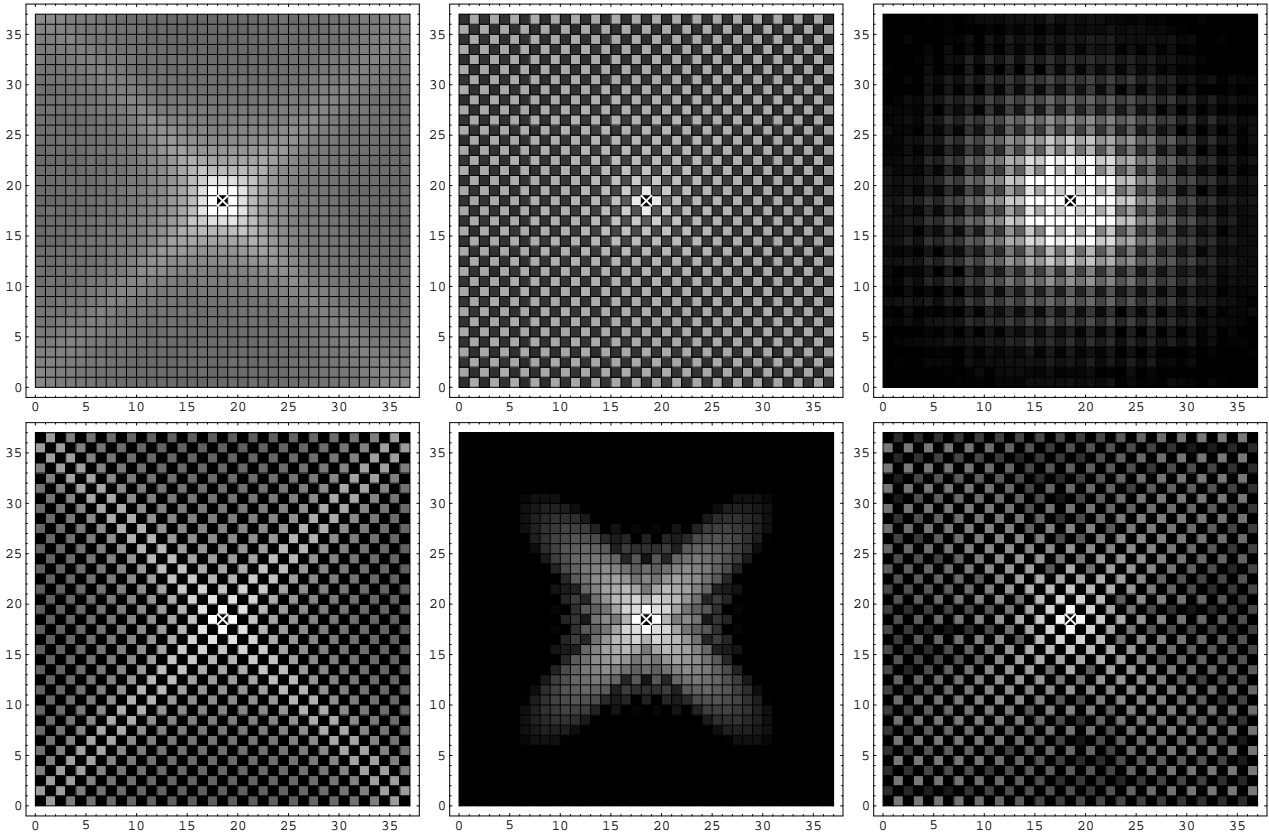


FIG. 4: **Top row:** VMC results for the hole density $n_h(m) = \langle (1 - n_m) \rangle_{\Psi'_l}$ (color coding: white/black correspond to high/low values of $n_h(m)$) in the partially projected state $|\Psi'_l\rangle$, for sites m other than the reservoir site l (marked by the cross). Left: Fermi sea. Middle: s -wave state. Right: d -wave state. **Second row:** Exact results for $d_h(m)$, see Eq. (28), in the unprojected state (color coding: white/black correspond to high/low values), for sites m other than the doubly occupied site l (marked by the cross). Left: Fermi sea. Middle: s -wave state. Right: d -wave state. **All:** The lattice has $37^2 + 1 = 1370$ sites and $n = 1$. For the BCS states, $\Delta = 1$.

tion. Here, we may expect deviations for quantities like the relative normalization X from the combinatorial result (10). Indeed, the VMC data presented in Fig. 2 confirms this expectation. For instance, the data show a qualitatively different dependence of X on doping, for the s -wave BCS states. The VMC data indicates a possibly different limiting behavior for X in the limit $n \rightarrow 1$, as indicated by the analysis of the data as a function of inverse cluster-size, presented in Fig. 3.

For the s -wave BCS state, we observe a dramatic enhancement in the double occupancy at the reservoir site for low doping, which we understand as a consequence of enhanced on-site pairing, relative to the Fermi liquid state. On the other hand, The double occupancy of the reservoir site is reduced for the d -wave, since the d -wave state suppresses on-site pairing fluctuations. The quantitative behavior of the normalization ratio X as a function of doping, for projected superconducting states is thus a subtle problem which we hope to solve in the future.

We also studied the hole density near the reservoir site for projected superconducting wave functions at half fill-

ing using VMC. The results are shown in the top row of Fig. 4. For the projected Fermi sea, we find that the hole density is uniform. However, for the superconducting states, we find that projection induces oscillations in the hole density near the reservoir site. For the projected d -wave state, we find that the hole density is mostly near the reservoir site. We believe that the Gutzwiller approximation needs to be extended to treat pairing correlations in the superconducting wave functions to understand these results fully. This issue, along with the study of systems away from half filling and their possible relevance to the checker-board pattern observed in scanning tunneling microscopy of the high temperature superconductors is left to future research.

We thank P.W. Anderson, N. P. Ong, and H. Yokoyama for several discussions. N.F. is supported by the Deutsche Forschungsgemeinschaft. V.N.M. acknowledges partial financial support from The City University of New York, PSC-CUNY Research Award Program.

-
- ¹ M. C. Gutzwiller, Phys. Rev. Lett. **10**, 159 (1963).
- ² K. Seiler, C. Gros, T.M. Rice, K. Ueda, D. Vollhardt, J. Low. Temp. Phys. **64**, 195 (1986).
- ³ C. Gros, R. Joynt, T.M. Rice, Phys. Rev. B **36**, 381 (1987).
- ⁴ P. W. Anderson, Science **235** 1196, (1987).
- ⁵ G. Baskaran, Z. Zou, and P. W. Anderson, Sol. State Commun. **63**, 973 (1987).
- ⁶ Claudio Gros, Phys. Rev. B **38**, 931 (1988).
- ⁷ F. C. Zhang, C. Gros, T. M. Rice and H. Shiba, Supercond. Sci. Tech. **1** 36 (1988); also available as cond-mat/0311604.
- ⁸ P. W. Anderson, P. A. Lee, M. Randeria, T. M. Rice, N. Trivedi and F. C. Zhang, J. Phys. Cond. Mat. **16** R755 (2004).
- ⁹ P. W. Anderson (private communication) and P. W. Anderson and N. P. Ong, cond-mat/0405518.
- ¹⁰ H. Yokoyama and H. Shiba, J. Phys. Soc. Jpn. **57**, 2482,(1988)
- ¹¹ A. Paramekanti, M. Randeria and N. Trivedi, Phys. Rev. Lett. **87** 217002 (2001); Phys. Rev. B **69** 144509 (2004); Phys. Rev. **70**, 054504 (2004).
- ¹² Masao Ogata, J.Phys. Soc. Jpn. **72**, 1839 (2003); also available as cond-mat/0304405.
- ¹³ Q.-H. Wang, D.-H. Lee and P. A. Lee Phys. Rev. B **69**, 092504 (2004).
- ¹⁴ D. Vollhardt, Rev. Mod. Phys. **56**, 99 (1984).
- ¹⁵ M. Randeria, R. Sensarma, N. Trivedi and F.-C. Zhang, cond-mat/0412096.
- ¹⁶ C. Gros, Annals of Physics **189**, 53 (1989).
- ¹⁷ However, we have indications that the hole is not bound to the reservoir site, since the density correlation seems to decay algebraically and because they decrease in magnitude with increasing lattice size.